

Molecular recognition in the solid state: topology of experimental and theoretical charge densities for tetrasulfur tetranitride†

Wolfgang Scherer,*^a Michael Spiegler,^a Bjørn Pedersen,^a Maxim Tafipolsky,^a Wolfgang Hieringer,^a Björn Reinhard,^a Anthony J. Downs^b and G. Sean McGrady*^c

^a Anorganisch-chemisches Institut der Technischen Universität München, Lichtenbergstraße 4, Garching bei München, D-85747 Germany

^b Inorganic Chemistry Laboratory, University of Oxford, South Parks Road, Oxford, UK OX1 3QR

^c Department of Chemistry, King's College London, Strand, London UK WC2R 2LS.

E-mail: sean.mcgrady@kcl.ac.uk

Received (in Cambridge, UK) 20th December 1999, Accepted 6th March 2000

Topological analysis of experimental and theoretical charge densities in tetrasulfur tetranitride clarifies features of the intramolecular bonding; intermolecular charge concentrations reveal directional 'key-lock' interactions corresponding to molecular recognition in the solid state.

Tetrasulfur tetranitride, S_4N_4 , is perhaps the most studied inorganic heterocycle, yet a full understanding of its bonding remains elusive. Thus, whilst S–S bonding interactions between proximal S atoms are established, the nature and extent of interaction remain unclear,^{1–3} and the existence of distal S...S interactions is either claimed^{1,4} or refuted.²

Two decades ago a low-temperature X-ray diffraction study provided the most accurate molecular geometry to date, and reported a preliminary analysis of the charge density distribution, $\rho(\mathbf{r})$, in S_4N_4 .¹ With the subsequent advances in instrumentation, analytical methods and computing power, we have undertaken experimental and theoretical studies of $\rho(\mathbf{r})$ for S_4N_4 ⁵ and a theoretical study of S_2N_2 for comparison. Our geometrical parameters for S_4N_4 are in good agreement with those of the earlier study.¹ We have clarified several inconsistencies still outstanding in the various bonding descriptions of S_4N_4 , and observed distortions in the experimental charge density giving rise to directional intermolecular attractions corresponding to molecular recognition in the solid state.

Intramolecular bonding: in order to reveal both gross and subtle features of $\rho(\mathbf{r})$, we have analysed its Laplacian, $\nabla^2\rho(\mathbf{r})$, using the 'Atoms in Molecules' (AIM) approach of Bader.⁶ By means of a topological analysis of $\rho(\mathbf{r})$, features such as bond critical points (CPs) and paths of maximum electron density can be used to construct a molecular graph representing the network of bond paths connecting linked atoms. As shown in Fig. 1(a), we find ten (3, –1) bond CPs,⁶ corresponding to eight S–N and two S–S linkages, and four (3, +1) ring CPs,⁶ in a tetrahedral array about a central (3, +3) cage CP.⁶ These conclusions are in accord with an earlier theoretical study.³ $\rho(\mathbf{r})$ at the cage CP is a minimum in all three dimensions, supporting the conclusions drawn from two theoretical deformation density studies,^{2,7} and affording no evidence of significant distal S...S interactions. The value of ρ at the bond CPs, $\rho(\mathbf{r}_c)$, for the S–S bonds [$\rho(\mathbf{r}_c)_{av} = 0.37(1) \text{ e } \text{Å}^{-3}$; av = average] is significantly lower than that for the S–N linkages [$\rho(\mathbf{r}_c)_{av} = 1.54(1) \text{ e } \text{Å}^{-3}$], being about one-third that reported for an S–S single bond.⁸ This, together with the long S–S distances⁸ of 2.5995(2) and 2.5950(2) Å and a positive value of the Laplacian,⁶ $\nabla^2\rho(\mathbf{r}_c)_{av} = 1.61(1) \text{ e } \text{Å}^{-5}$, may be interpreted in terms of a weak, closed-

shell interaction between the two S atoms. However, analysis of both kinetic energy densities $G(\mathbf{r})$ and potential energy densities $V(\mathbf{r})$ ¹⁰ of the electrons at the bond critical points suggests some covalent character for the S–S bond [$H(\mathbf{r}_c) = G(\mathbf{r}_c) + V(\mathbf{r}_c) = -0.116$; $G(\mathbf{r}_c) = 0.228 \text{ hartree } \text{Å}^{-3}$].⁹

The shortness of the S–N bond [1.629(1) Å; on average] and its degree of ellipticity⁶ [$\epsilon = 0.17$; $\rho(\mathbf{r}_c)_{av} = 1.54(1) \text{ e } \text{Å}^{-3}$; $\nabla^2\rho(\mathbf{r}_c)_{av} = -10.60(3) \text{ e } \text{Å}^{-5}$] implies π -contributions. The bond paths are displaced, respectively, outwards and inwards for the S–S and S–N bonds, and the S–N bond CPs are located closer to the electropositive S atoms [Fig. 1(a)]. Calculated atomic charges¹¹ suggest transfer of ca. 1.3 electrons to N from S, although monopole charges based on the X-ray multipolar model suggest a lower figure of 0.3 electrons.

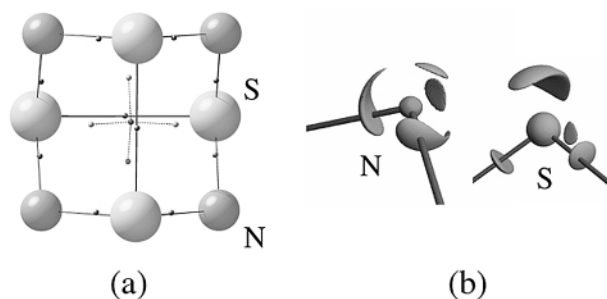


Fig. 1 (a) Location of the critical points denoted by closed circles in the S_4N_4 skeleton. The bond critical points along the S–N bonds are shifted towards the more electropositive sulfur atoms. Important distances (Å) and angles (°) (average values): S–N 1.629(1), S–S 2.598(1); N–S–N 104.5(1), S–N–S 112.7(1). (b) Isosurface maps at constant $-\nabla^2\rho(\mathbf{r})$ values indicating bonded and non-bonded charge concentrations on N(1) and S(2) [$-\nabla^2\rho(\mathbf{r}) = 45$ and $9 \text{ e } \text{Å}^{-5}$, respectively].

Intermolecular bonding. The solid-state structure of S_4N_4 consists of helical chains of molecular units along the crystallographic b -axis. The pronounced polarity of the S–N bonds orients neighbouring molecules such that electrostatic S...N contacts are formed [Fig. 2(a),(b)]. $\rho(\mathbf{r})$ at the intermolecular S...N bond CPs is rather small [$\rho(\mathbf{r}_c)_{av} = 0.085(1) \text{ e } \text{Å}^{-3}$], but is substantially greater than, for example, the S...S intramolecular interactions in 3,3,6,6-tetramethyl-S-tetathiane [$\rho(\mathbf{r}_c) = 0.043(1) \text{ e } \text{Å}^{-3}$].¹² Despite the flatness of the $\rho(\mathbf{r})$ map, four intermolecular bond CPs, six ring CPs and one cage CP have been located; all experimental and theoretical topological parameters are in good agreement. A more detailed picture emerges from analysis of the Laplacian, $\nabla^2\rho(\mathbf{r}_c)$, in regions corresponding to these intermolecular bonding interactions. The results are depicted in Fig. 2 as contour plots for (a) the NNS'S', and (b) the SNN'S' interactions, respectively. Here maxima in $-\nabla^2\rho(\mathbf{r}_c)$ signal regions of local charge concentration and minima regions of local charge depletion. In accord with both the present and an earlier theoretical study,³ we deduce that (i)

† Electronic supplementary information (ESI) available: experimental details; listing of geometrical and topological parameters; fractional atomic coordinates and mean square atomic displacement parameters; multipole population coefficients; expansion and contraction coefficients; description of the local coordinate systems and basis set information. See <http://www.rsc.org/suppdata/cc/a9/a910209o/>

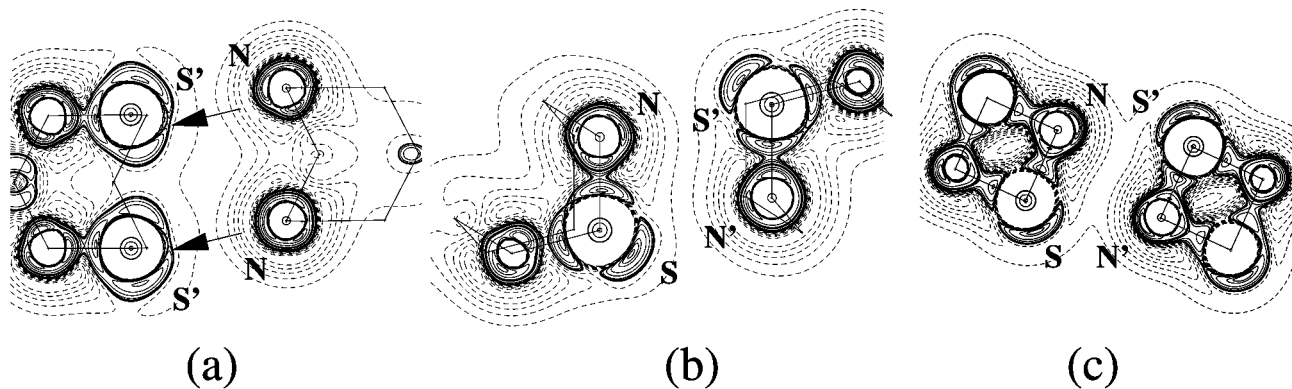


Fig. 2 Contour plots of charge concentrations determined experimentally and by calculation [B3LYP/6-311G(3df) level]. Negative values of $-\nabla^2\rho(r)$ are marked by broken lines. (a) $-\nabla^2\rho(r)_{\text{exp}}$ in the NNS'S' plane and (b) $-\nabla^2\rho(r)_{\text{exp}}$ in the SNN'S' plane. The relative orientations of the S_4N_4 molecules are indicated by solid lines. Salient distances (Å) and angles ($^\circ$): S–N' 3.0882(8); N–S···N' 79.43(3); N···NS' 100.00(3). (c) $-\nabla^2\rho(r)_{\text{calc}}$ in the SNN'S' plane of the $(S_2N_2)_2$ dimer. In (a) the 'key-lock' interaction is marked by arrows.

two bonded and two non-bonded, and (ii) three bonded and one non-bonded charge concentrations, respectively, in the valence shells of the N and S atoms of S_4N_4 are retained in the solid state [Fig. 1(b)].

While the bonded charge concentrations constitute the intramolecular bonds, the *magnitude* and *location* of the non-bonded charge concentrations on the nitrogen and the local charge depletions on the sulfur atoms should be responsible for the orientation of the S_4N_4 molecules in the solid state.^{3,13} According to a point charge model, optimal interaction should occur for closest contact of S···N' pairs, giving a value of 90° for the NNS' angle in the NNS'S' plane. In fact, this angle is $100.00(3)^\circ$ on account of the directionality of the interactions between the local charge concentrations in the valence shells of the N atom and the associated regions of charge depletion on the corresponding S' atom. Fig. 2 clearly shows the resulting 'key-lock' principle of facing charge concentrations and charge depletions in the valence shells of the nitrogen and sulfur atoms in the intermolecular NNS'S' plane of the $(S_4N_4)_2$ dimer. A similar pattern of charge tessellation is displayed by the Laplacian in the corresponding NSN'S' plane of S_4N_4 and also in the structurally related model system $(S_2N_2)_2$,¹² as depicted in Fig. 2(c). For $(S_2N_2)_2$ the S···N' contacts are significantly shorter than in $(S_4N_4)_2$ [2.890(1)¹⁴ cf. 3.0882(8) Å], in accord with the proclivity of S_2N_2 to polymerise to $(SN)_x$ with the transformation of one S···N' contact into a covalent S–N bond.

The 'key-lock' interaction based on the Laplacian goes beyond a point charge model which takes no account of the polarisation of the valence shell and the consequent formation of local charge concentrations and depletions. Whilst crystal architecture is often controlled by directional interactions like hydrogen bonding,¹⁷ this appears to be the first experimental study to reveal a simple three-dimensional directional interaction involving facing charge concentrations and charge depletions as a transferable architectural principle in a molecular crystal. The transferability of the 'key-lock' pattern is remarkable since S_2N_2 and S_4N_4 display rather different geometries and electronic structures. These results suggest that similar architectural forces encoded in the Laplacian of the charge density may be more generally revealed by this type of experimental study. The ability to observe such intermolecular interactions is an important advance, for it demonstrates the response of the non-isolated molecule to its chemical environment, and so holds out the prospect of a better understanding not just of molecular structure, but of molecular *reactivity* and molecular *recognition* under appropriate conditions.

Notes and references

- 1 M. L. DeLucia and P. Coppens, *Inorg. Chem.*, 1978, **17**, 2336.
- 2 A. S. Brown and V. H. Smith, Jr., *J. Chem. Phys.*, 1993, **99**, 1837.

- 3 T.-H. Tang, R. F. W. Bader and P. J. MacDougall, *Inorg. Chem.*, 1985, **24**, 2047.
- 4 M. J. Almond, G. A. Forsyth, D. A. Rice, A. J. Downs, T. L. Jeffery and K. Hagen, *Polyhedron*, 1989, **8**, 2631.
- 5 *Crystal data* for S_4N_4 : $M_r = 184.32$, yellow prisms; monoclinic, space group $P2_1/n$, $a = 8.7286(4)$, $b = 7.0783(4)$, $c = 8.6377(4)$ Å, $\beta = 93.722(2)^\circ$, $V = 532.54(5)$ Å³; $T = 100(1)$ K; $Z = 4$, $F(000) = 368$, $D_c = 2.299$ g cm⁻³, $\mu = 16.6$ cm⁻¹. 32220 (22404) Bragg reflections were collected on a Nonius kappa-CCD system with a rotating anode generator (Nonius FR591; Mo-K α , radiation ($\lambda = 0.71073$ Å)); data for a second crystal in parentheses); 6887 (5488) independent reflections were observed. Both data sets were independently corrected for beam inhomogeneity and absorption effects and scaled together: 99.8% completeness in the data range $\sin\theta/\lambda_{\text{max}} = 1.10$ Å⁻¹; $R_{\text{int}} = 0.028$ for 6108 unique reflections. The deformation density was described by a multipole model in terms of spherical harmonics multiplied by Slater-type radial functions with energy-optimised exponents (see ref. 16). The multipole expansion was terminated at the hexadecapolar level. The refinement of 105 parameters against 4849 observed reflections [$F > 3\sigma(F)$] converged to $R_1 = 0.025$, $wR_2 = 0.033$, GOF = 1.62, and a featureless residual $\rho(r)$. CCDC 182/1565. See <http://www.rsc.org/suppdata/cc/a9/a910209o/> for crystallographic files in .cif format.
- 6 R. F. W. Bader, *Atoms in Molecules—A Quantum Theory*, Clarendon Press, Oxford, 1990.
- 7 Experimental deformation densities from this study also display a minimum in $\Delta\rho(r)$ at the centre of the S_4N_4 cage.
- 8 *Ab initio* molecular orbital calculations on H_2S_2 and S_2 suggest reference charge densities at the bond CP of 0.999 and 1.389 e Å⁻³ for single and double S–S bonds, respectively; see ref. 13.
- 9 $G(r)$ values are computed from experimental $\rho(r)$ values using the approach from Yu. A. Abramov, *Acta Crystallogr., Sect. A.*, 1997, **53**, 264.
- 10 D. Cremer and E. Kraka, *Angew. Chem., Int. Ed. Engl.*, 1984, **23**, 627.
- 11 All calculations were performed at the B3LYP/6-311G(3df) level using Gaussian 98. The geometries of S_4N_4 , $(S_4N_4)_2$ and $(S_2N_2)_2$ were fixed at the experimentally determined ones. The topology of $\rho(r)_{\text{calc}}$ was analysed using the AIM software package (ref. 15).
- 12 K. L. McCormack, P. R. Mallinson, B. C. Webster and D. S. Yufit, *J. Chem. Soc., Faraday Trans.*, 1996, **92**, 1709.
- 13 A similar key-lock situation based on an experimental charge density study has been observed in the case of the van der Waals interactions between two chlorine atoms in the (100) plane of solid Cl_2 ; see: V. G. Tsirelson, P. F. Zou, T.-H. Tang and R. F. W. Bader, *Acta Crystallogr., Sect. A.*, 1995, **51**, 143.
- 14 M. J. Cohen, A. F. Garito, A. J. Heeger, A. G. MacDiarmid, C. M. Mikulski, M. S. Saran and J. Kleppinger, *J. Am. Chem. Soc.*, 1976, **98**, 3844.
- 15 R. F. W. Bader, *Acc. Chem. Res.*, 1985, **18**, 9.
- 16 E. Clementi and C. Roetti, *At. Data Nucl. Data Tables*, 1974, **14**, 177; N. K. Hansen and P. Coppens, *Acta Crystallogr., Sect. A.*, 1978, **34**, 909; T. Koritsánszky, S. Howard, T. Richter, Z. W. Su, P. R. Mallinson and N. K. Hansen, *XD—A Computer Program Package for Multipole Refinement and Analysis of Electron Densities from Diffraction Data*, Free University of Berlin, Germany, 1995.
- 17 See, for example, D. Braga, F. Grepioni and G. R. Desiraju, *Chem. Rev.*, 1998, **98**, 1375.

Communication a910209o